Potential to Detect Small KBO Stellar Occultations with CubeSats

Savanna Guertin[a], Mike Bottom[b]

[a]*Sacramento State University, 6000 J St, Sacramento, CA 95819*

[b]*Institute for Astronomy, University of Hawai'i, 2680 Woodlawn Drive, Honolulu, HI 96822, USA*

Abstract

Different formation models of the solar system make significantly varying predictions for the size distributions of small (~1 km) Kuiper belt objects (KBOs). However, determining this size distribution is challenging because these small objects are extremely faint, so unable to be directly detected, and are expected to pass in front of a target star once every century. Currently only ~4 potential occultation events have been reported over the years. To detect a substantial number of small KBOs requires specialized equipment with wide fields and extremely fast photometers. Single mission concepts like *Whipple* have the challenge of dealing with high false positive and data rates. Recently, a revolution in satellite designs like CubeSats and SmallSats has allowed for specialized science missions at lower costs. In this work we determine the potential for CubeSats or SmallSats to work as specialized KBO occultation detectors. Using data from recent CubeSat missions and commercially available, flight-qualified hardware, we perform numerical simulations to determine detection rates for small KBO occultations. We simulate with aperture sizes from CubeSats to SmallSats at a range of observational bands. We determine that while CubeSats of 6-12 cm apertures are not able to meaningfully detect KBOs, 25 cm apertures would be able to increase the number of detected KBOs by ~30 over a two-year observational period.

Keywords: *occultations, CubeSats*

1. Introduction

In the distant outskirts of our solar system lies the Kuiper Belt, ranging from 30 to 50 AU from the Sun. It is estimated to have tens of thousands of Kuiper Belt Objects (KBOs) larger than 100 km in diameter and millions of small objects with diameters of 20 km down to sub-km objects. Models and observation suggest that the size distribution of KBOs follows a broken power law, with collisions modifying the size distribution between the power laws for large and small KBOs (Kenyon & Bromley 2004; Pan & Sari 2005). Having detailed constraints on the

Email address: savannaguertin@csus.edu (Savanna Guertin)

August 2, 2020

size distribution of these objects would allow for insight into the initial planetesimal population of the Kuiper Belt. Currently, over a thousand KBOs larger than 15 km have been discovered but objects smaller than 10 km are too faint ($\geq 35^{th}$ magnitude) to be directly detected (Pass et al. 2017). While there have been a few detections of small KBOs, there are not enough detections to determine the slope of the power law.

Although small KBOs cannot be directly imaged, they can be inferred from serendipitous stellar occultations (Bailey 1976). As the object passes in front of a background star, there can be a rapid drop in the star's light. The main source of the motion driving the timescale of the occultation is the orbital motion of the Earth (Nihei et al. 2007), and with characteristic timescales of less than one second. When a KBO is smaller than the Fresnel scale, defined as $\sqrt{\lambda a/2}$, the occultation event will be dominated by diffraction effects. With occultations of small KBOs being observable only briefly, rapid photometry is required. Therefore, the sampling rate is a critical parameter for an occultation survey since a single KBO may only pass in front of a star once a century, making follow-ups not feasible. Bickerton et al. (2009) found the Nyquist sampling rate (minimum sample rate to adequately recover the signal) for detection of a KBO at 40 AU in the optical is 40 Hz.

Not only is a fast sampling rate needed to detect these occultations of small KBOs, the signal must be strong enough to overcome noise from the detector and other sources. This will require low read noise detectors and continuous monitoring of a wide number of stars, due to the rarity of an event. While monitoring many stars is desired, it is also important to look towards the ecliptic, where KBOs are more likely to pass in front of a star. Ground-based programs have a serious additional photometric obstacle due to atmospheric scintillation (Stefannson et al. 2017).

So far, there have been few occultation candidate events for small KBOs for both ground and space-based surveys. For ground surveys, the challenge of scintillation makes large dish sizes almost mandatory and with the added difficulty of receiving substantial observing time on these large telescopes, detecting a small KBO occultation is rare. In recent years new instruments have been developed for ground-based detections of small KBOs. Specifically, CHIMERA was developed for use at the prime focus of the Hale 200-inch telescope with simultaneous optical imaging in two bands to combat false positive rates (Harding et al. 2016). Also recently developed, Colibri is a dedicated KBO occultation robotic telescope array using two independent electron-multiplying charge coupled device (EMCCD) cameras (Pass et al. 2017). Arimatsu et al. (2019) reported an occultation event candidate by a KBO with a radius of ~1.3 km, observed simultaneously with two amateur telescopes. Schlichting et al. (2009) analyzed 12,000 star hours, sampled at 40 Hz, from the Hubble Space Telescope fine guidance sensor (a rapid photometer used to stabilize the pointing of the observatory), and reported a potential observed occultation by an object with a ~500 m radius at a distance

of 45 AU. A second occultation candidate event, corresponding to a ~530 m object, was reported after analysis of an additional 19,500 star hours (Schlichting et al. 2012). Chang et al. (2011) analyzed a total of 240 kilo-seconds (ks) of data taken by the Proportional Counter Array onboard *Rossi X-ray Timing Explorer (RXTE)* from Sco X-1 (the brightest X-ray source in the sky) with only one dip event found. Detections with a single camera are challenging as the false positive rates are difficult to determine, and the inability to follow-up the objects makes it crucial to be confident in a true detection.

The need for fast photometry and continuous observation of many stars makes occultation detection missions ill-suited to general observatory platforms, which have broad scope covering many science areas. Back in 2011, *Whipple* was a proposed space observatory in the NASA Discovery Program with a dedicated plan to detect stellar occultations of distant objects (Alcock et al.). The satellite would use a 77-centimeter aperture telescope with a quick sampling rate of 40 Hz, simultaneously observing ~40,000 stars. Although the detections results looked promising, the costs of the mission and false positive rates were a challenge.

Recently, a small revolution has occurred in satellite design driven by the advent of small, modular spacecraft known as CubeSats. Together with their larger counterpart, SmallSats, these spacecraft have been largely enabled by a drop in launch prices. This drop in launch costs is due in part to the use of reusable rockets and the ability for many CubeSats to fly as ancillary cargos through various CubeSat launch initiatives. In recent years market forces are evolving for developing rockets meant only for small cargo (CubeSats, SmallSats, etc.), like the Electron (up to 150 kg), at launch prices of only ~6m, an order of magnitude less than the ~40m launch price of a Pegasus.

CubeSats are a class of nanosatellites that use a standard size known as 1U (one unit) measuring 10x10x10 cm which can be extended up to 12U. NASA's CubeSat Launch Initiative provides opportunities for small payloads built by universities, high schools, and non-profit organizations to fly on upcoming launches. SmallSats are a more general class of small satellites, varying in sizes with the microsatellite class ranging from 10–100 kg.

Currently scientific CubeSats are used more for terrestrial remote sensing, since most astrophysical observations require good pointing control and large apertures. However, there has been an investment by NASA to mature the CubeSat concept for focused, independent, small-to-medium scale scientific observations. In recent years missions like the Colorado Ultraviolet Transit Experiment (CUTE) and PicSat are working towards using CubeSats to execute specialized astrophysical science observations. There is also a surge in using multiple CubeSats or SmallSats, known as constellations. One challenge for CubeSats and SmallSats is that pointing errors result in an independent noise floor for space-based observations, similar to scintillation for ground-based telescopes (Knapp et al. 2020). However, the Arcsecond Space Telescope Enabling Research in Astrophysics (ASTERIA) was a technology demonstration and science mission to

conduct astrophysical measurements using a CubeSat, with the goal of reducing systematic photometric noise. ASTERIA demonstrated precision photometry at 1000 ppm with only a 6 cm aperture, matching the performance of significantly larger ground telescopes. With the use of CubeSat constellations, false positive rates can be almost be entirely mitigated.

Additionally, recent advances in detectors have demonstrated extremely low read noise necessary for rapid photometry. This includes the development of large-format scientific CMOS devices (Bai et al. 2008) capable of megapixel readouts at ~50Hz with sub-electron read noise, and EMCCDs like the CCD201-20 (Daigle et al. 2018). In the infrared, linear-mode avalanche photodiode devices such as the SAPHIRA arrays (Atkinson et al. 2018) are approaching these levels of performance as well, demonstrating sub-electron readout noise and extremely low dark current rates on ~0.1 megapixel devices. While the EMCCDs and LmAPD devices, which are more recent developments, are only beginning to be space-qualified, the CMOS devices now have wide usage in spacecraft.

With the advent of these detectors, coupled with the growing ubiquity of CubeSats, this motivates a reassessment of the potential to detect meaningful amounts of small KBO occultations that *Whipple* was aiming for. The lack of scintillation, few limits to continuous observing, and lowered launch costs, a CubeSat or SmallSat may be a feasible option for a occultation survey. The CubeSat constellation concept allows for multi-telescope mission profiles that were previously only realistic on the ground. When both telescopes trigger a detection within a second of each other (to accommodate telescope separation), a flag is raised and the data surrounding the occultation is stored for later downlinking to Earth.

In this paper we will be assessing the potential of a CubeSat or SmallSat to detect occultations of stars by small KBOs with ~1 km diameter. We will use both numerical modeling and experimental data to determine the required photometric parameters to perform these observations. This will require comparing the total noise for ground telescopes and space telescopes based on telescope diameter and stellar magnitude. Assessment of survey yield will be performed to determine how many occultations are expected to be seen and what limits on the size distribution could be placed using a CubeSat.

---

2. Method

2.1 Simulating Occultation Curves

To understand how well a CubeSat will be able to detect small KBOs occultations, we need to simulate realistic occultation light curves to work with. When a KBO is smaller than the Fresnel scale (~1.3 km at 40 AU), defined as $\sqrt{\lambda a/2}$, the occultation event will be

dominated by diffraction effects. When the object passes directly in front of the background star, described as having an impact parameter of 0, the diffraction effects are easily seen. The diffraction pattern of these events is described using Lommel functions as shown in detail by Nihei et al. (2007). As the impact parameter increases, the depth of the occultation event becomes quite small. Figure 1 shows the effect of the impact parameter on an occultation event. With every parameter the same, except the impact parameter, it is clear to see how big an effect it has on the shape of the light curve.

To test the potential of using a SmallSat for detecting stellar occultations from small KBOs, we first need a variety of pristine light curves. We use the Colibri pipeline from Pass et al. (2017) to generate noiseless occultation curves for various parameters as shown in Table 1.

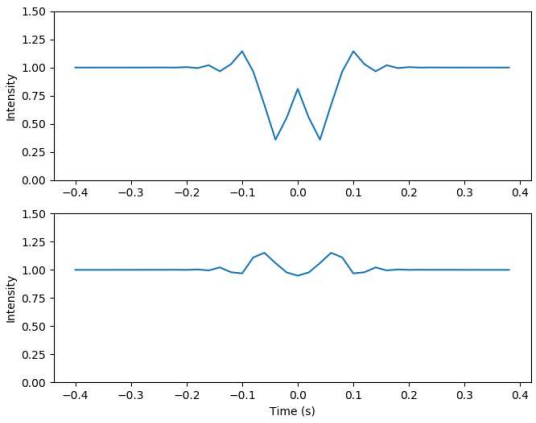

Figure 1: Intensity curves for an occultation pattern with two different impact parameters. Top: 2 km occulter with 0 impact parameter. Bottom: 2 km occulter with 2 km impact parameter.

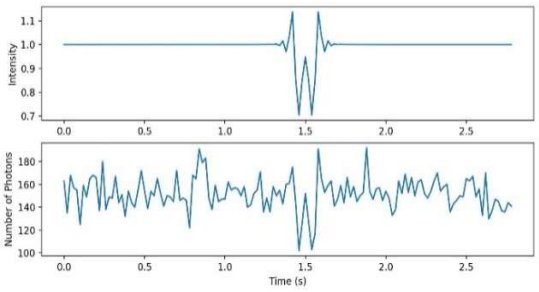

Figure 2: Occultation profile, sampled at 50 Hz, from a 1000 m occulting KBO with a 0 m impact parameter in V-band. Top is noiseless and bottom is with photon noise of an 8 V-mag star and 25 cm aperture.

The different parameters that go into the occultation modeling and the effects of those parameters include:

- *KBO diameter (m):* The larger the occulting object, the depth of the event in the light curve increases.
- *Stellar angular diameter (mas):* As the angular size of the target star increases, it smooths out the diffraction pattern and can decrease the occultation depth.
- *Impact parameter (m):* This parameter has one of the largest effects on the occultation profile as seen in Figure 1. If the object does not pass directly in front of the star, the shape of the light curve changes drastically.
- *Arbitrary Shift Adjustment:* Modeled occultation patterns are dependent on the time at which exposures were centered, so an arbitrary shift adjust was added with respect to the middle of the exposure (Pass et al. 2017).
- *Sampling Rate (Hz):* The number of samples per second determine how detailed the occultation curve signal can be. If the sampling rate is too slow (around 5 Hz), there will be no sign an occultation event

ever happened. Diffraction features are only clearly visible around a 40 Hz sampling rate.

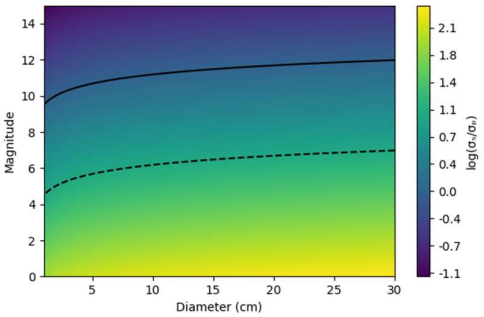

Figure 3: The ratio of scintillation noise to photon noise in the magnitude-telescope-diameter plane for ground-based telescopes, assuming a perfect telescope and airmass of 1.0. The solid curve shows where the scintillation noise equals shot noise. Stars below the solid line are scintillation limited, and above are photon limited. The dashed curve shows

With 2,240 curves for each UBVRI filter, there is a wide variety of occultation profiles that we will compare to one another. The occultation profiles are generated in 50 second chunks. We then add four different types of noise that would affect a space-based occultation mission:

- *Photon/shot noise (photons)*: Caused by inherent fluctuations in the light from stars that can be modeled by a Poisson process. The amount of shot noise depends on the aperture size, optical efficiency/throughput, and star brightness.
- *Read noise (e-/pixel)*: Generated by the electronics as the charge present in the pixels in transferred to the camera.
- *Dark current (e-/s/pixel)*: Arises from the thermal energy within the detector, creating electrons over time and being detected as signal.
- *Systematic noise*: From either detector or spacecraft (e.g, jitter), it only allows for a certain amount of photometric accuracy.

Figure 2 shows a noiseless occultation profile generated from the Colibri pipeline and the same curve with only photon noise added. As seen, the occultation dip is still easily identifiable with a bright 8 V-mag star and 25 cm aperture.

2.2 Noise

While EMCCD and LmAPD detectors can potentially exceed the performance of CMOS detectors, they are not at the same stage of flight qualification, and in the latter case would require complex cryogenic cooling. As such, we baseline commercially available, space-qualified CMOS detectors, such as the Teledyne DALSA's IC-47-12288-00-R, which have typical read noise of 3 to 5e-/frame, and dark current rates of 50e/s at operating temperatures of 25 C. We estimate the efficiency for the different filters based on quantum efficiency curves provided by the manufacturer as, 20% for U-band, 30% for I-band, 75% for B-band, 80% for the V-band, and 95% for R-band. For detector noise we simulate with 0-5 e read noise, up to 50 e/s of dark current, and up to 10% systematic noise. Our systematic noise assumptions are derived from extrapolation of ASTERIA noise data to short exposure times down to 0.01 s (Figure 6; Knapp et al. 2020). We do not include any astrophysical noise (e.g. rotation and granulation) since there is no

known noise from those sources at our small timescales. With these parameters in place we will determine the estimated detection numbers and false positives rates over a 2-year mission observing time with all the described input parameters.

To detect these small KBO occultations, observation of bright stars is needed. It is useful to analyze the advantage of a space telescope being free of scintillation noise compared to a ground telescope of the same size. We compare the ratio of scintillation noise to photon noise based on telescope diameter and stellar magnitude as seen in Figure 3. The estimated scintillation noise σ_s for a given star is described by Young (1967) and Dravins et al. (1998) in units of relative flux,

$$\sigma_s = 0.09 D^{-\frac{2}{3}} x^{1.75} \left(2t_{\exp}\right)^{-\frac{1}{2}} e^{\frac{-h}{h_0}}$$

where D is the diameter of the telescope in centimeters, x is the airmass of the observation, $t_{\exp}$ is the exposure time in seconds, h is the altitude of the observatory in meters, and h_0 is the atmospheric scale height set to 8000 m. The constant 0.09 has a unit of $\mathrm{cm}^{\frac{2}{3}}\mathrm{s}^{\frac{1}{2}}$, such that the scintillation error is in units of relative flux.

Figure 3 shows that small telescopes with diameters 30 cm or less are scintillation limited up to ~10 V-mag stars. We also compared the total noise (only assuming photon and scintillation noise) of a ground and space telescope at quick exposure times with a small aperture (10 cm). We found that even when assuming an Airmass value of 1.0 and not including seeing or other noise that affects ground-based telescopes, at exposure times around 0.01 s, a space telescope will have ~50% less total noise.

2.3 Detection Rates and False Positives

We implemented a simple detection algorithm to test with the simulated occultation light curves. The method does not need any information on the shape or depth of the occultation profile. This detection algorithm could be performed on board the spacecraft and save only the data points where a candidate event is flagged. The implemented algorithm scans across the light curves, taking the mean and standard deviation of the flux over a long window consisting of 20 seconds of data points. If the current point goes a conservative 3.75σ above or below the mean, a flag is set and the algorithm then waits to see if the next three data points also include a 3.75σ peak or dip (same as what was flagged). If so, a detection is triggered, and the time of the second data point is saved for extraction of the light curve.

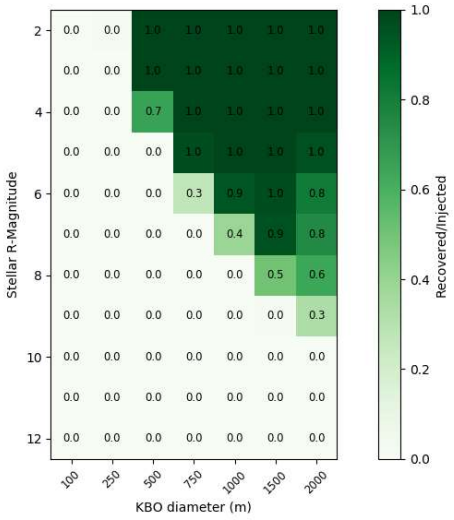

Figure 4: Detection rates based on stellar R-magnitude and KBO diameter. The plot used has two 25cm aperture telescopes assuming only shot noise and a 50 Hz sampling rate.

This algorithm is simple enough that analytic false positive rates can be estimated and compared with numerical simulations of the output from the algorithm. We calculated the false positive rate for one telescope which yielded one false positive every 5 days per star with one telescope. Then we simulated false positive rates by running our detection algorithm with a 5-day, noisy light curve input for each stellar magnitude. Our numerical simulations for false positive rates were consistent with the analytic calculations up to 11th magnitude, where photon counts are too low at a 50 Hz sampling rate. After we determined our numerical simulations were consistent with the analytic expectation, we simulated false positive counts over a two-year observing period with two telescopes, which confirmed that false positives can be almost entirely mitigated.

Using two small, identical satellites effectively screens out false positives while retaining nearly the same true positive rate. While adding a second satellite will increase mission cost, the costs are usually driven by development and engineering costs (Ardila et al. 2019), not hardware costs. Therefore, constructing a second identical spacecraft would only marginally affect the total cost of the mission. Preliminary simulations indicated a very low detection efficiency for satellites with apertures smaller than 12 cm. Therefore, we focused our analysis on satellites with aperture of 12 and 25 cm, corresponding to either large CubeSats or SmallSats.

We consider a detection to be simultaneous if it occurs on both telescopes within one second to accommodate for spacecraft separation. Figure 4 shows the detection rates from two telescopes with 100 injected occultation curves per bin, each with randomized KBO and stellar parameters. Based on the use of two identical 25 cm aperture telescopes, assuming only photon noise, the detection rate drops off significantly at ~10 R-mag for a 2000 m KBO. When using two 12 cm aperture telescopes, there is a 0% detection rate for all KBO sizes by 8th V-mag and dimmer.

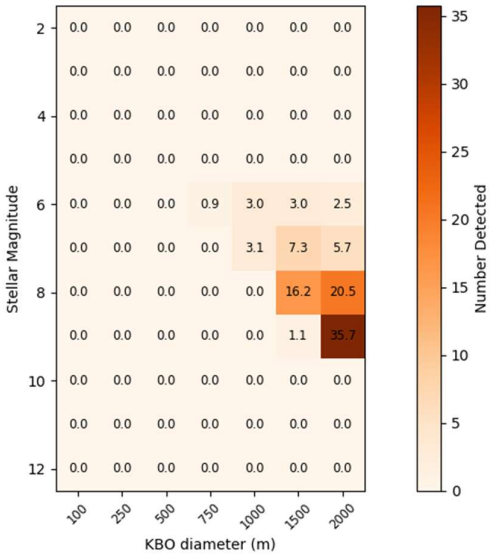

Figure 5: Field detection numbers based on stellar R-magnitude and KBO diameter. These numbers use the detections rates in Figure 4 and a 10 deg^2 field area simulated star counts from TRILEGAL 1.6.

2.4 Expected Event Rates

Using the expected average time between KBO occultations based on the minimal detectable diameter with a q_s = 2 power law index (Figure 4; Bickerton et al. 2009), which has a weak wavelength dependence that we ignore, we simulated the expected number of detections during a given observational time and star field. We decided to simulate with a conservative 10 deg^2 field of view (FOV) even though ASTERIA, with a 6 cm

aperture, has 11.2x9.6 deg^2 FOV (Knapp et al. 2020). We use TRILEGAL 1.6 to simulate realistic star fields at the position where the galactic center and ecliptic intersect, α= 18.5 h and δ= -23.3 deg (Vanhollebeke et al. 2009). From the 2 deg^2 field area star counts, we extrapolated to have a 10 deg^2 field area. The total number of stars in the field (brighter than 12th R-magnitude) we end up with is 3,500.

Taking the efficiency that were outputted from our detection algorithm in Section 2.3, we simulate how many total detections there would be over a 24-month observational period.

3. Results

Our best results were attained in R-band with a total of ~32 total detections with 3 e of read noise, 50 e/s dark current rate, and 5% systematic noise. If there is only shot noise, the R-band detections increase to around 95 in two years as shown in Figure 5. It is important to note that the star counts and quantum efficiencies based on wavelength play a significant role in the number of detections from these results, with B-band and V-band being feasible options for observing.

Figure 6 shows the false positive counts over a 2-year observational period. When simulating with two telescopes there were 0 false counts until 11 V-mag, where photon counts are almost zero at a 50 Hz sampling rate. The results comparing two 12 cm vs. 25 cm apertures with different noise values and all UBVRI filters are shown in Table 2.

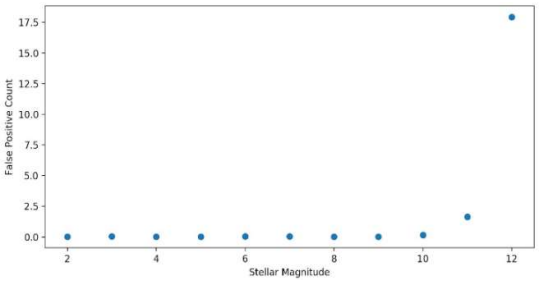

Figure 6: False positive counts over a 2-year observational period for V-band stellar magnitudes using two 25 cm telescopes at 50 Hz sampling rate.

4. Conclusion

To be able determine the power-law index of the size distribution for small Kuiper Belt Objects, we need detections of these (~1 km) objects. Currently, only ~4 detections of potential small KBO occultation events have been reported over the past years. In 2011, *Whipple* was a proposed space observatory with the goal of detecting these small objects using a large, 77 cm aperture telescope at a 40 Hz sampling rate. The mission concept faced the challenge of high expenses and high false positive and data rates. With lowered launch costs and a surge in the use of small satellites today, it is important to reevaluate the potential to detect small KBOs with space-based telescopes. Especially currently, the use of two small telescopes is becoming a feasible option for space missions. In this work we compared the detection efficiency between using two 12 cm or 25 cm aperture telescopes.

The results show that two 12 cm telescopes may be too small to be effective and worth an occultation mission. However, when the apertures are increased to 25 cm the detection numbers look promising and the telescope size is still feasible for a SmallSat mission. While our results show that R-band has the most detection numbers, we believe that is only caused by the simulated star counts we

used. B and V-band both have relatively high quantum efficiencies and produced satisfactory detection numbers.

With these results, future work can be done to go into more detail on the costs and potential mission design. If detector noise continues to be minimized and/or eliminated, detection numbers can almost triple when there is only shot noise involved.

Acknowledgements

Savanna Guertin acknowledges support from the Research Experience for Undergraduate program at the Institute for Astronomy, University of Hawaii-Manoa funded through NSF grant 6104374.

Savanna Guertin would like to thank the Institute of Astronomy for their kind hospitality during the course of this project.

We would like to thank Leon K. Harding from the Center for Space Science and Engineering Research at Virginia Tech for providing useful feedback and discussions throughout the project.

KBO diameter (m)	Stellar Angular Diameter (mas)	Impact Parameter (m)	Shift Adjustment	Sampling Interval (Hz)
[100, 250, 500, 750, 1000, 1500, 2000]	[0.001, 0.005, 0.01, 0.03, 0.08]	[0, $R/2$, R, $2R$] *	[0, 0.1, 0.25, 0.5]	[100, 50, 25, 12.5]

Table 1: Input parameters used for generating occultation profiles using the Colibri pipeline (Pass et al. 2017).

*Where R is the KBO radius (m).

Band Filter	Aperture Size (cm)	Read Noise (e/frame)	Dark Current Rate (e/s)	Systematic Noise (%)	Number of Detections
U	12	0	0	0	1.2
	25	0	0	0	13.8
	12	3	50	5	0.0
	25	3	50	5	4.6
B	12	0	0	0	10.8
	25	0	0	0	91.7
	12	3	50	5	3.1
	25	3	50	5	32.6
V	12	0	0	0	6.0
	25	0	0	0	58.4
	12	3	50	5	3.0
	25	3	50	5	22.9
R	12	0	0	0	9.6
	25	0	0	0	99.0
	12	3	50	5	3.5
	25	3	50	5	37.2
I	12	0	0	0	0.7
	25	0	0	0	14.8
	12	3	50	5	0.0
	25	3	50	5	5.7

Table 2: Field Detection results showing the number of total detections over a two-year observing period. Compares the impact of detector noise and aperture sizes.

Email address: savannaguertin@csus.edu (Savanna Guertin)

References

Alcock, C., Holman, M., Lehner, M., Murray, S., Protopapas, P., & Werner, M. Whipple: Exploring the solar system beyond Neptune using a survey for occultations of bright stars.

Ardila, D. R., Freeman, A., Gaier, T., Gorjian, V., Shkolnik, E., & Wolk, S. (2019). Astro2020 APC White Paper: SmallSats for Astrophysics. *arXiv preprint arXiv:1909.13747*.

Arimatsu, K., Tsumura, K., Usui, F., Shinnaka, Y., Ichikawa, K., Ootsubo, T., ... & Watanabe, J. (2019). A kilometre-sized Kuiper belt object discovered by stellar occultation using amateur telescopes. Nature Astronomy, 3(4), 301-306.

Atkinson, D., Hall, D., Jacobson, S., & Baker, I. M. (2018). Photon-counting properties of saphira apd arrays. *The Astronomical Journal*, *155*(5), 220.

Bai, Y., Bajaj, J., Beletic, J. W., Farris, M. C., Joshi, A., Lauxtermann, S., ... & Williams, G. (2008, July). Teledyne imaging sensors: silicon CMOS imaging technologies for x-ray, UV, visible, and near infrared. In *High energy, optical, and infrared detectors for astronomy III* (Vol. 7021, p. 702102). International Society for Optics and Photonics.

Bailey, M. E. (1976). Can 'invisible'bodies be observed in the Solar System?. Nature, 259(5541), 290-291.

Bickerton, S. J., Welch, D. L., & Kavelaars, J. J. (2009). Kuiper Belt Object Occultations: Expected Rates, False Positives, and Survey Design. The Astronomical Journal, 137(5), 4270.

Daigle, O., Turcotte, J., Djazovski, O., Gloutnay, É., Grandmont, F., Veilleux, J., ... & Thibault, S. (2018, July). TRL-5 EMCCD controller for space applications. In *Space Telescopes and Instrumentation 2018: Optical, Infrared, and Millimeter Wave* (Vol. 10698, p. 106986E). International Society for Optics and Photonics.

Harding, L. K., Hallinan, G., Milburn, J., Gardner, P., Konidaris, N., Singh, N., ... & Schlichting, H. E. (2016). CHIMERA: a wide-field, multi-colour, high-speed photometer at the prime focus of the Hale telescope. *Monthly Notices of the Royal Astronomical Society*, *457*(3), 3036-3049.

Iuzzolino, M., Accardo, D., Rufino, G., Oliva, E., Tozzi, A., & Schipani, P. (2017). A cubesat payload for exoplanet detection. Sensors, 17(3), 493.

Knapp, M., Seager, S., Demory, B. O., Krishnamurthy, A., Smith, M. W., Pong, C. M., ... & Smith, C. (2020). Demonstrating high-precision photometry with a CubeSat: ASTERIA observations of 55 Cancri e. arXiv preprint arXiv:2005.14155.

Kenyon, S. J., & Bromley, B. C. (2004). The size distribution of Kuiper belt objects. The Astronomical Journal, 128(4), 1916.

Pan, M. (2005). Shaping the Kuiper belt size distribution by shattering large but strengthless bodies. Icarus, 173(2), 342-348.

Email address: savannaguertin@csus.edu (Savanna Guertin)

Pass, E., Metchev, S., Brown, P., & Beauchemin, S. (2017). Pipeline for the detection of serendipitous stellar occultations by Kuiper belt objects with the Colibri fast-photometry array. arXiv preprint arXiv:1711.00358.

Nihei, T. C., Lehner, M. J., Bianco, F. B., King, S. K., Giammarco, J. M., & Alcock, C. (2007). Detectability of occultations of stars by objects in the Kuiper belt and Oort cloud. The Astronomical Journal, 134(4), 1596.

Osborn, J., Föhring, D., Dhillon, V. S., & Wilson, R. W. (2015). Atmospheric scintillation in astronomical photometry. Monthly Notices of the Royal Astronomical Society, 452(2), 1707-1716.

Schlichting, H. E., Ofek, E. O., Nelan, E. P., Gal-Yam, A., Wenz, M., Muirhead, P., ... & Livio, M. (2012). Measuring the abundance of sub-kilometer-sized Kuiper belt objects using stellar occultations. The Astrophysical Journal, 761(2), 150.

Schlichting, H. E., Ofek, E. O., Wenz, M., Sari, R., Gal-Yam, A., Livio, M., ... & Zucker, S. (2009). A single sub-kilometre Kuiper belt object from a stellar occultation in archival data. Nature, 462(7275), 895-897.

Stefansson, G., Mahadevan, S., Hebb, L., Wisniewski, J., Huehnerhoff, J., Morris, B., ... & Knutson, H. (2017). Toward Space-like Photometric Precision from the Ground with Beam-shaping Diffusers. The Astrophysical Journal, 848(1), 9.

Vanhollebeke, E., Groenewegen, M. A. T., & Girardi, L. (2009). Stellar populations in the Galactic bulge-Modelling the Galactic bulge with TRILEGAL. Astronomy & Astrophysics, 498(1), 95-107.

Appendix